ORIGINAL PAPER

Diazabicyclo[2.2.2]octane stabilized on Fe_3O_4 as catalysts for synthesis of coumarin under solvent-free conditions

Mohammad Ali Nasseri · Seyed Mohsen Sadeghzadeh

Abstract Fe_3O_4-diazabicyclo[2.2.2]octane (Fe_3O_4-DAB-CO) magnetic nanoparticles (MNPs) catalyst was readily prepared from inexpensive starting materials in aqueous media which catalyzed the synthesis of coumarin. FTIR spectroscopy, X-ray diffraction, transmission electron micrographs were employed to characterize the properties of the synthesized Fe_3O_4-DABCO MNPs. High catalytic activity and ease of recovery from the reaction mixture using external magnet, and several reuse times without significant losses in performance are additional eco-friendly attributes of this catalytic system.

Keywords Fe_3O_4-DABCO · Coumarin · Magnetic nanoparticles (MNPs) · Green chemistry · One-pot synthesis

Introduction

In recent years, core–shell multi-components have attracted intense attention because of their potential applications in catalysis [1]. Different from single-component that can only supply people with one function, the core–shell multi-components can integrate multiple functions into one system for specific applications [2–6]. Moreover, the interactions between different components can greatly improve the performance of the multi-components system and even generate new synergetic properties. Among the core–shell structured composites, the composites with magnetic core and functional shell structures have received especial attention because of their potential applications in catalysis, drug storage/release, selective separation, chromatography, and chemical or biologic sensors [7–12]. The magnetic core has good magnetic responsibility, and can be easily magnetized. Therefore, the composites with magnetic core can be conveniently collected, separated or fixed by external magnet.

1,4-Diazabicyclo[2.2.2]octane (DABCO), a cage-like compound, is a small diazabicyclic molecule with weak alkalescency and medium-hindrance [13]. DABCO has been applied as an inexpensive, eco-friendly, high reactive and non-toxic base catalyst for various organic transformations, including ring opening of aziridines with amines or thiols [14], oxidative deprotection of (tetrahydropyranyl) ethers and silyl ethers [15], conversion of tetrahydropyranyl ethers into acetates [16], regioselective nucleophilic aromatic substitution reaction [17], synthesis of isoxazolines [18], synthesis of N-arylphthalimides [19], synthesis of industrially important polyurethane foams [20], and Baylis–Hillman reactions [21, 22]. Nevertheless, in many of these cases, DABCO has not been recovered, and eliminated as a residue.

Herein we report the fabrication of DABCO incorporated into a surface magnetite nanoparticles which catalyzed the synthesis coumarin under solvent-free conditions. The prepared Fe_3O_4-DABCO MNPs are multi-functional. The Fe_3O_4 core makes them very easy to be separated and recycled from solution with the help of an external magnet (Scheme 1).

Experimental

Materials and methods

Chemical materials were purchased from Fluka and Merck in high purity. Melting points were determined in open

M. A. Nasseri (✉) · S. M. Sadeghzadeh
Department of Chemistry, College of Sciences, University of Birjand, P.O. Box 97175-615, Birjand, Iran
e-mail: mohammadali.nasseri@yahoo.com;
manaseri@birjand.ac.ir

Scheme 1 Synthesis of coumarin from phenol and ethyl acetoacetate in the presence of Fe$_3$O$_4$-DABCO
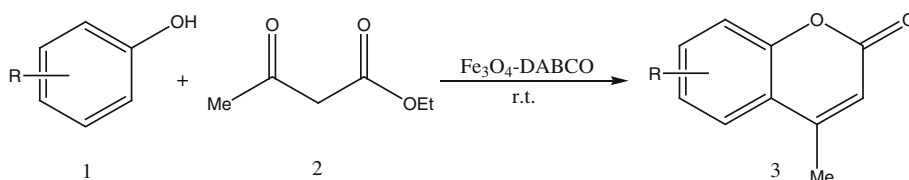
capillaries using an Electrothermal 9100 apparatus and are uncorrected. Powder X-ray diffraction data were obtained using Bruker D8 advance model with Cu ka radiation. FTIR spectra were recorded on a VERTEX 70 spectrometer (Bruker) in the transmission mode in spectroscopic grade KBr pellets for all the powders. The particle size and structure were observed by using a Philips CM10 transmission electron microscope operating at 100 kV. The thermo-gravimetric analysis (TGA) curves were recorded under air atmosphere using TGA/DTA Shimadzu-50 with platinum pan. The samples were heated in air from 25 to 1,000 °C with a heating rate of 10 °C/min. The weight losses as a function of temperature were recorded. NMR spectra were recorded in DMSO on a Bruker advance DRX-400 MHz instrument spectrometer using TMS as internal standard. The purity determination of the products and reaction monitoring were accomplished by TLC on silica gel polygram SILG/UV 254 plates. Mass spectra were recorded on Shimadzu GCMS-QP5050 mass spectrometer.

General procedure for the preparation of Fe$_3$O$_4$ nanoparticles

The synthesis procedure is illustrated as follows: (1) 0.01 mol FeCl$_2$·4H$_2$O and 0.03 mol FeCl$_3$·6H$_2$O were dissolved into 200 mL distilled water, followed by the addition of PEG (1.0 g, MW 6,000), (2) sodium hydroxide (NaOH) was added to the solution and the pH value was controlled in the range $12 \leq \text{pH} \leq 13$, and (3) different amount of hydrazine hydrate (N$_2$H$_4$·H$_2$O, 80 % concentration) was added to the above suspension. The reaction was continued for about 24 h at room temperature. During this period, the pH value was adjusted by NaOH and kept in the range of $12 \leq \text{pH} \leq 13$. The black Fe$_3O_4$ NPs were then rinsed several times with ionized water.

General procedure for the preparation of n-propyl-4-aza-1-azoniabicyclo[2.2.2]octane

2 mmol DABCO and 2 mL THF were mixed together in a beaker, and then 2 mmol of NaH was dispersed into the mixture by ultrasonication. 2.5 mmol 3-chloropropyl-triethoxysilane was added drop-wise at room temperature and stirred for another 16 h at 60 °C. The resultant products were collected and washed with ethanol and deionized

water in sequence, and then dried under vacuum at 60 °C for 2 h for further use.

General procedure for the preparation of Fe$_3$O$_4$-DABCO

For the synthesis of Fe$_3$O$_4$-DABCO MNPs, 2 mmol of Fe$_3$O$_4$ MNPs was dispersed in a mixture of 80 mL of ethanol, 20 mL of deionized water and 2.0 mL of 28 wt% concentrated ammonia aqueous solution (NH$_3$·H$_2$O), followed by the addition of 20 mmol of compound n-propyl-4-aza-1-azoniabicyclo[2.2.2]octane. After vigorous stirring for 24 h, the final suspension was repeatedly washed, filtered for several times and dried at 60 °C in the air.

General procedure for the synthesis of coumarin

A mixture of phenol (1 mmol), ethyl acetoacetate (1 mmol), and Fe$_3$O$_4$-DABCO MNPs (0.0007 g) was stirred at 90 °C for 35–45 min. EtOH was added to the reaction mixture and the Fe$_3$O$_4$-DABCO MNPs were separated by external magnet. Then the solvent was removed from solution under reduced pressure and the resulting product was purified by recrystallization using ethanol.

Results and discussion

Due to the reasonable needs to clean and green recovery of the heterogenous catalyst, we synthesized Fe$_3$O$_4$-DABCO as a new catalyst nanomagnetic iron oxide simply (Fig. 1). The synthesized Fe$_3$O$_4$-DABCO was then characterized by different methods such as X-ray power diffraction (XRD), transmission electron microscopy (TEM), and FTIR.

XRD

The structural properties of synthesized Fe$_3$O$_4$-DABCO nanoparticle were analyzed by XRD. As shown in Fig. 2, XRD patterns of the synthesized Fe$_3$O$_4$-DABCO nanoparticle display several relatively strong reflection peaks in the 2θ region of 20–80°, which is quite similar to those of Fe$_3$O$_4$ nanoparticles reported by other group. The discernible six diffraction peaks in Fig. 2 can be indexed to (220), (311), (400), (422), (511), and (440), which match

Fig. 1 Schematic illustration of the synthesis for Fe_3O_4-DABCO MNPs
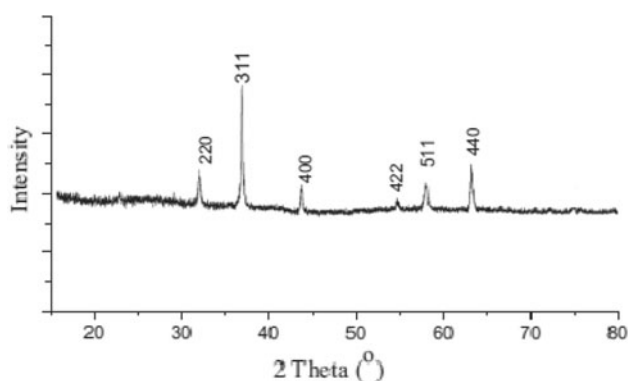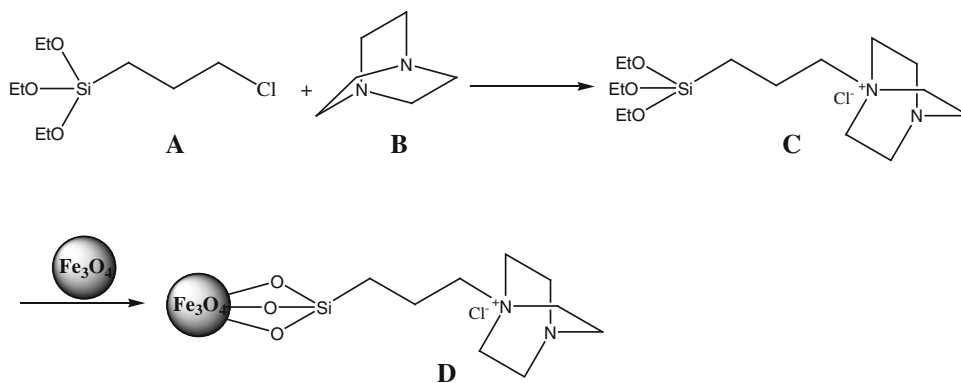
Fig. 2 XRD analysis of Fe_3O_4-DABCO MNPs

well with the database of magnetite in JCPDS (JCPDS Card: 19-629) file.

TEM

The size and structure of the Fe_3O_4-DABCO were also evaluated using TEM (Fig. 3a, b). From TEM images (Fig. 3b), it can be seen that Fe_3O_4 MNPs are uniformly coated with DABCO layer. The average size of Fe_3O_4 MNPs is about 15–25 nm (Fig. 3a). After being coated with a DABCO, the typical core–shell structure of the Fe_3O_4-DABCO can be observed, and the average size increases to about 40–50 nm (Fig. 3b).

FTIR

The successful conjugation of DABCO onto the surface of the Fe_3O_4 nanoparticles was confirmed by the FTIR spectra (Fig. 4). The peaks at 3,415 and 590 cm^{-1} appear in all the FTIR spectra, which are assigned to the –OH group and the Fe–O group, respectively (Fig. 4a). In FTIR spectra of the Fe_3O_4-DABCO MNPs, the C–N$^+$ stretching at 1,615 cm^{-1}, CH$_2$ bending at 1,480 cm^{-1}, Si–C stretching at 1,210 cm^{-1}, and Si–O stretching at 1,110–1,090 cm^{-1} are observed as a broad band (Fig. 4b).

TGA

The thermal behavior of Fe_3O_4-DABCO MNPs is shown in Fig. 5. This was evaluated to be 1.5 % according to the TG analysis. The analysis showed two decreasing peaks. First peak appears at temperature around 130–150 °C due to desorption of water molecules from the catalyst surface. This is followed by a second peak at 425–450 °C, corresponding to the loss of the organic spacer group (Fig. 5). According to the TGA, the amount of DABCO functionalized on Fe_3O_4 is evaluated to be 2.2 mmol g^{-1}.

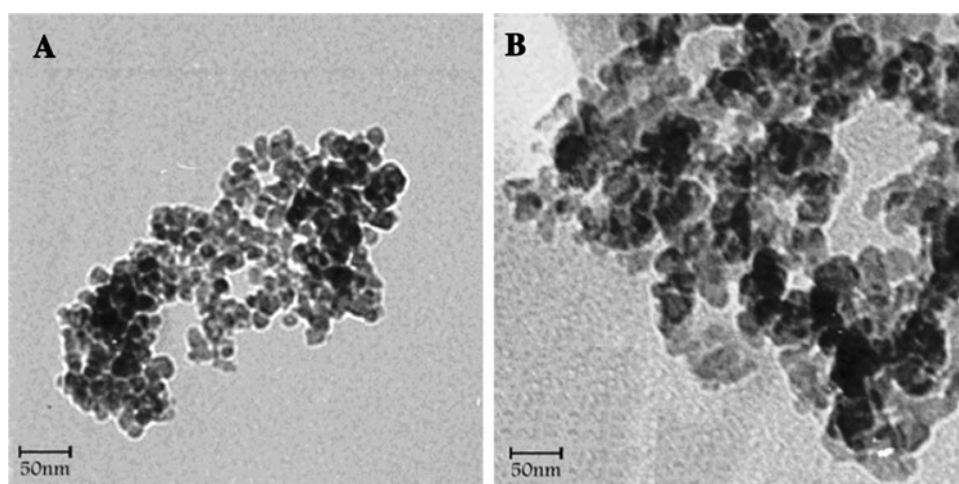## Catalytic activity of Fe_3O_4-DABCO MNPs for the one-pot synthesis of coumarin

We thought to optimize the reaction conditions; the same reaction was carried out in various solvents under similar conditions. In this study, it was found that solvent-free is a more efficient and superior solvent (Table 1, entry 14) over other solvents (Table 1, entries 1–13) with respect to reaction time and yield of the desired coumarin.

At this stage, the amount of catalyst necessary to promote the reaction efficiently was examined (Fig. 6). It was observed that the variation for Fe_3O_4-DABCO MNP had an effective influence. The best amount of Fe_3O_4-DABCO MNP is 0.0007 g which afforded the desired product in 93 % yields (Fig. 6).

Under the optimal conditions, the reaction progress in the presence of 0.0007 g of Fe_3O_4-DABCO MNPs was monitored by GC (Fig. 7). Using this catalyst system, excellent yields of coumarin can be achieved in 35 min at 90 °C. No apparent by-products were observed by GC in all the experiments and the cyclic carbonate was obtained cleanly in 93 % yield.

It is important to note that the magnetic property of Fe_3O_4-DABCO MNPs facilitates its efficient recovery from the reaction mixture during work-up procedure. The activity of the recycled catalyst was also examined under the optimized conditions. After the completion of reaction, the catalyst was separated by an external magnet, washed

Fig. 3 TEM images of **a** Fe$_3$O$_4$, **b** Fe$_3$O$_4$-DABCO MNPs

Fig. 4 FTIR spectra of **a** Fe$_3$O$_4$, **b** Fe$_3$O$_4$-DABCO MNPs
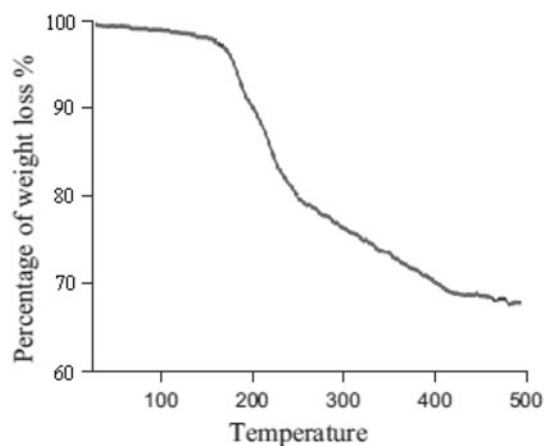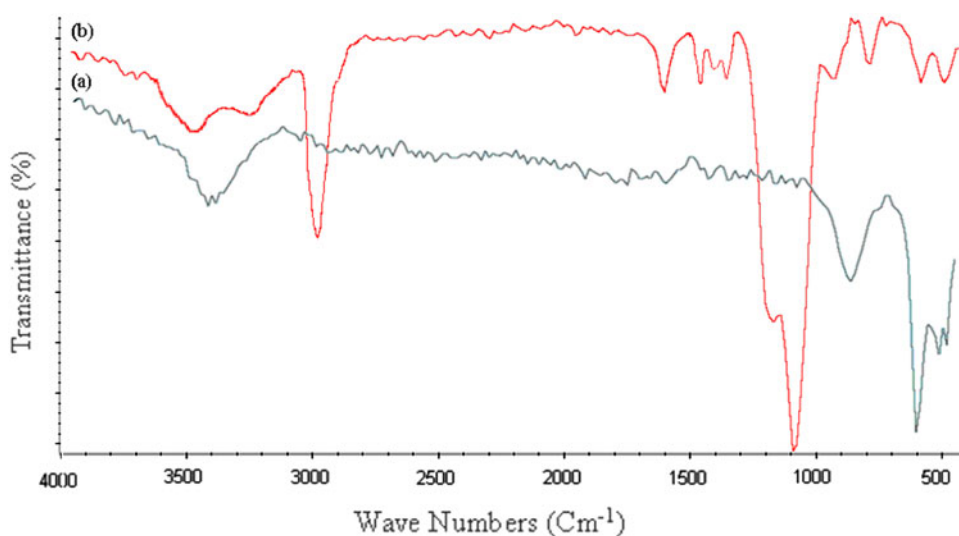
Fig. 5 TGA diagram of Fe$_3$O$_4$-DABCO MNPs

with methanol and dried at the pump. The recovered catalyst was reused for six consecutive cycles without any significant loss in catalytic activity (Fig. 8).

In order to show the unique catalytic behavior of Fe$_3$O$_4$-DABCO MNPs in these reactions, we have performed one-pot reaction of phenol and ethyl acetoacetate in the presence of a catalytic amount of H$_3$PW$_{12}$O$_{40}$, NbCl$_5$, PEG-SO$_3$H, InCl$_3$, Pd(PPh$_3$)$_4$, cerium(IV) ammonium nitrate, nano-SiO$_2$, nano-RuO$_2$, nano-TiO$_2$, nano-Fe$_3$O$_4$, nano γ-Fe$_2$O$_3$, and nano-FeNi$_3$ (Table 2). As it is evident from Table 2, Fe$_3$O$_4$-DABCO MNP is the most effective catalyst for this purpose, leading to the formation of coumarin in a good yield.

After optimization of the reaction conditions, this methodology was evaluated using variety of different substituted phenol in the presence of nanocatalyst under similar conditions. The reaction proceeded smoothly and was completed for 35–50 min at 90 °C (Table 3).
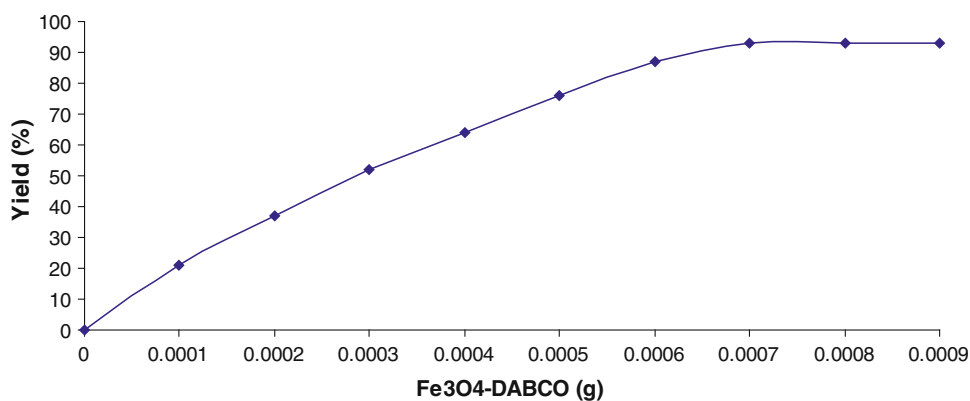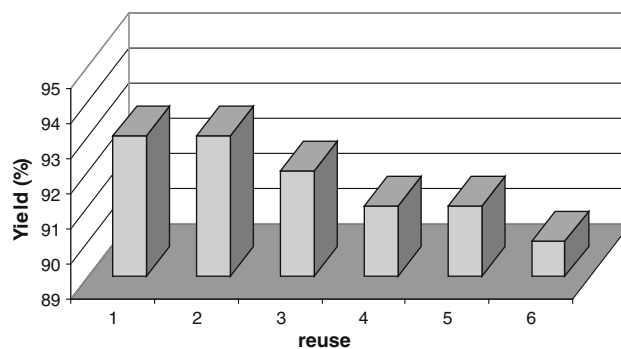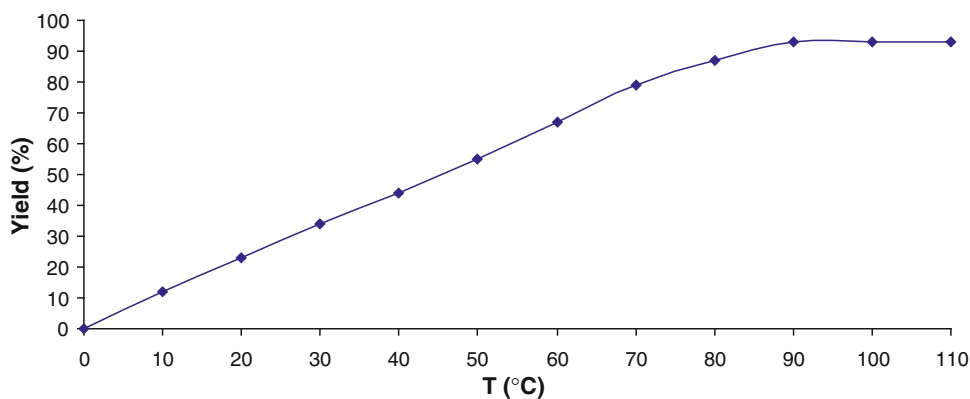
A plausible mechanism for the reaction between phenol and ethyl acetoacetate on Fe$_3$O$_4$-DABCO MNPs surface during the synthesis of coumarin is depicted in Scheme 2. The Fe$_3$O$_4$-DABCO MNP has lewis acid and lewis basic sites.

Table 1 Solvent screening for the reaction between phenol and ethyl acetoacetate

Entry	Solvent	Yield (%)[a]
1	H_2O	79
2	EtOH	64
3	CH_3CN	53
4	THF	34
5	CH_2Cl_2	28
6	Toluene	20
7	EtOAC	63
8	*n*-Hexane	Trace
9	$CHCl_3$	Trace
10	DMSO	48
11	MeOH	55
12	Dioxane	Trace
13	DMF	49
14	Solvent-free condition	93

Reaction conditions: phenol (1 mmol), ethyl acetoacetate (1 mmol), solvent (10 ml), Fe_3O_4-DABCO MNPs (0.001 g) at 100 °C for 40 min

[a] Isolated yields

Fig. 8 Reuse performance of the catalysts

Selected spectroscopic data

Compound (**3a**): IR (KBr): υ cm^{-1}: 3162, 1684, 1379, 1225, 1059, 973, 849, 750, 580, 532, 436. ^{1}H NMR: δ 10.50 (brs, 1H), 7.54–7.51 (d, $J = 9$ Hz, 1H), 6.77–6.74 (d, $J = 8$ Hz, 1H), 6.66 (s, 1H), 6.07 (brs, 1H), 2.31 (brs, 3H). ^{13}C NMR: δ 161.58, 160.69, 155.25, 153.81, 126.89, 113.25, 112.42, 110.67, 102.57, 18.46.

Fig. 6 Effect of increasing amount of Fe_3O_4-DABCO MNPs on the preparation of coumarin (reaction of phenol and ethyl acetoacetate in the presence of Fe_3O_4-DABCO MNPs at 100 °C)

Fig. 7 Reaction progress monitored by GC

Table 2 Comparison of the catalytic efficiency of Fe$_3$O$_4$-DABCO with various catalysts

Entry	Catalyst	Time (min)	Yield (%)[a]
1	Fe$_3$O$_4$-DABCO MNP	50	93
2	H$_3$PW$_{12}$O$_{40}$	50	32
3	NbCl$_5$	50	Trace
4	PEG-SO$_3$H	50	Trace
5	InCl$_3$	50	25
6	Pd (PPh$_3$)$_4$	50	38
7	Cerium (IV), ammonium nitrate	50	Trace
8	Nano-SiO$_2$	50	46
9	Nano-RuO$_2$	50	55
10	Nano-TiO$_2$	50	48
11	Nano-Fe$_3$O$_4$	50	59
12	Nano γ-Fe$_2$O$_3$	50	63
13	Nano-FeNi$_3$	50	65

[a] Phenol (1 mmol), ethyl acetoacetate (1 mmol) at 90 °C for 35 min

Table 3 Synthesis of coumarin derivatives catalyzed by Fe$_3$O$_4$-DABCO MNPs

Product	R	Time (min)	Yield (%)
3a	3-OH	35	93
3b	2,3-(OH)$_2$	35	97
3c	3,5-(OH)$_2$	35	95
3d	2-Me-3-OH	45	96
3e	3-Me-5-OH	40	93
3f	3-Me	40	90
3g	3-MeO	35	95
3h	3,5-(Me)$_2$	45	83
3i	3-NH$_2$	40	86
3g	1-Naphthol	45	85
3k	4-OH	35	89

[a] Reaction condition: phenol (1 mmol), ethyl acetoacetate (1 mmol), Fe$_3$O$_4$-DABCO MNPs (0.0007 g) at 90 °C

[b] Yield refers to isolated product

Compound (**3b**): IR (KBr): υ cm^{-1}: 3445, 1866, 1678, 1610, 1519, 1453, 1362, 1283, 1184, 1050, 1005, 956, 851, 808, 758, 718, 643, 605, 508. ^{1}H NMR: δ 9.10–10.13 (brs, 2H), 7.07–7.04 (d, J = 8.5 Hz, 1H), 6.80–6.77 (d, J = 8.5 Hz, 1H), 6.10 (s, 1H), 2.32 (s, 3H). ^{13}C NMR: δ 160.65, 154.31, 149.86, 143.78, 132.60, 115.89, 113.23, 112.57, 110.64, 18.65.

Compound (**3c**): IR (KBr): υ cm^{-1}: 3491, 3167, 1619, 1465, 1363, 1295, 1158, 1070, 1017, 919, 830, 757, 665, 546. ^{1}H NMR: δ 10.50 (s, 1H), 10.28 (s, 1H), 6.23 (brs, 1H), 6.14 (brs, 1H), 5.81 (s, 1H), 2.46 (s, 3H). ^{13}C NMR: δ 161.48, 160.55, 158.36, 156.92, 155.40, 109.28, 102.51, 99.48, 94.95, 23.86.

Compound (**3d**): IR (KBr): υ cm^{-1}: 3198, 2925, 1684, 1568, 1372, 1308, 1082, 953, 857, 805, 731, 598, 539. ^{1}H NMR: δ 10.34 (s, 1H), 7.39–7.36 (d, J = 8.75 Hz, 1H), 6.83–6.80 (d, J = 8.5 Hz, 1H), 6.06 (s, 1H), 2.31 (s, 3H), 2.11 (s, 3H). ^{13}C NMR: δ 160.85, 159.30, 154.09, 153.23, 123.47, 112.35, 112.06, 111.08, 110.30, 18.54, 11.20.

Compound (**3e**): IR (KBr): υ cm^{-1}: 3263, 1608, 1446, 1373, 1152, 1084, 976, 910, 832, 685, 536. ^{1}H NMR: δ 10.45 (s, 1H), 6.56 (s, 1H), 6.53 (s, 1H), 5.99 (s, 1H), 2.50 (s, 3H), 2.24 (s, 1H). ^{13}C NMR: δ 160.25, 156.86, 155.74, 155.21, 143.13, 111.97, 108.14, 106.93, 101.35, 24.32, 21.56.

Compound (**3f**): IR (KBr): υ cm^{-1}: 3054, 1712, 1613, 1386, 1322, 1264, 1190, 1142, 1019, 952, 877, 805, 753, 710, 571, 524, 437. ^{1}H NMR: δ 7.65–7.62 (d, J = 8.25 Hz, 1H), 7.20 (brs, 1H), 7.17 (s, 1H), 6.30 (s, 1H), 2.39 (br, 6H). ^{13}C NMR: δ 160.39, 153.68, 153.44, 143.22, 125.83, 125.50, 117.64, 116.90, 113.73, 21.46, 18.46.

Compound (**3g**): IR (KBr): υ cm^{-1}: 2953, 1724, 1619, 1512, 1454, 1383, 1279, 1209, 1148, 1067, 1019, 975, 857, 798, 748, 707, 633, 528, 491, 454. ^{1}H NMR: δ 7.68–7.64 (d, J = 8.5 Hz, 1H), 6.96 (s, 1H), 6.93–6.92 (d, J = 2.5 Hz, 1H), 6.19 (s, 1H), 3.84 (s, 3H), 2.38 (s, 3H). ^{13}C NMR: δ 162.83, 160.61, 155.24, 153.86, 126.91, 113.52, 112.57, 111.53, 101.16, 56.34, 18.57.

Compound (**3h**): IR (KBr): υ cm^{-1}: 2924, 1729, 1650, 1384, 1080, 849. ^{1}H NMR: δ 7.105 (s, 1H), 6.979 (s, 1H), 6.135 (s, 1H), 2.317 (s, 3H), 2.148 (s, 3H), 1.300–1.217 (brs, 3H). ^{13}C NMR: δ 164.60, 160.18, 154.76, 142.11, 137.51, 129.85, 115.82, 115.02, 111.60, 24.73, 19.49, 14.77.

Compound (**3i**): IR (KBr): υ cm^{-1}: 3437, 3350, 3243, 1616, 1540, 1445, 1395, 1260, 1212, 1154, 1057, 834, 709, 639, 529, 453. ^{1}H NMR: δ 7.393–7.359 (d, J = 8.5 Hz, 1H), 6.562–6.527 (dd, J = 6 Hz, J = 2.25 Hz, 1H), 6.388–6.379 (d, J = 2.25 Hz, 1H), 6.068 (brs, 2H), 5.877–5.873 (s, 1H), 2.276–2.272 (s, 3H). ^{13}C NMR: δ 161.16, 155.90, 154.18. 153.51, 126.63, 111.60, 109.28, 107.91, 98.96, 18.44.

Compound (**3j**): IR (KBr): υ cm^{-1}: 2919, 1712, 1464, 1373, 1168, 1079, 941, 847, 809, 745, 563. ^{1}H NMR: δ 8.36–8.32 (m, 1H), 8.04-8.00 (m, 1H), 7.86–7.65 (m, 4H), 6.48 (s, 1H), 2.51 (s, 3H). ^{13}C NMR: δ 160.09, 154.62, 134.81, 129.09, 128.41, 127.82, 124.36, 122.65, 122.06, 121.69, 115.54, 114.29, 19.10.

Compound (**3k**): ^{1}H NMR: δ 9.71 (s, 1H), 7.22–7.19 (brs, 1H), 7.00 (br, 2H), 6.33 (s, 1H), 2.34 (s, 3H). ^{13}C NMR: δ 160.49, 154.19, 153.21, 146.64, 120.61, 120.23, 117.75, 114.93, 109.98, 18.49.

Conclusions

In conclusion, we have developed the current important areas of heterogenization of DABCO, which is a rapidly

Scheme 2 Plausible
mechanism for the synthesis of
coumarin on Fe_3O_4-DABCO
surface
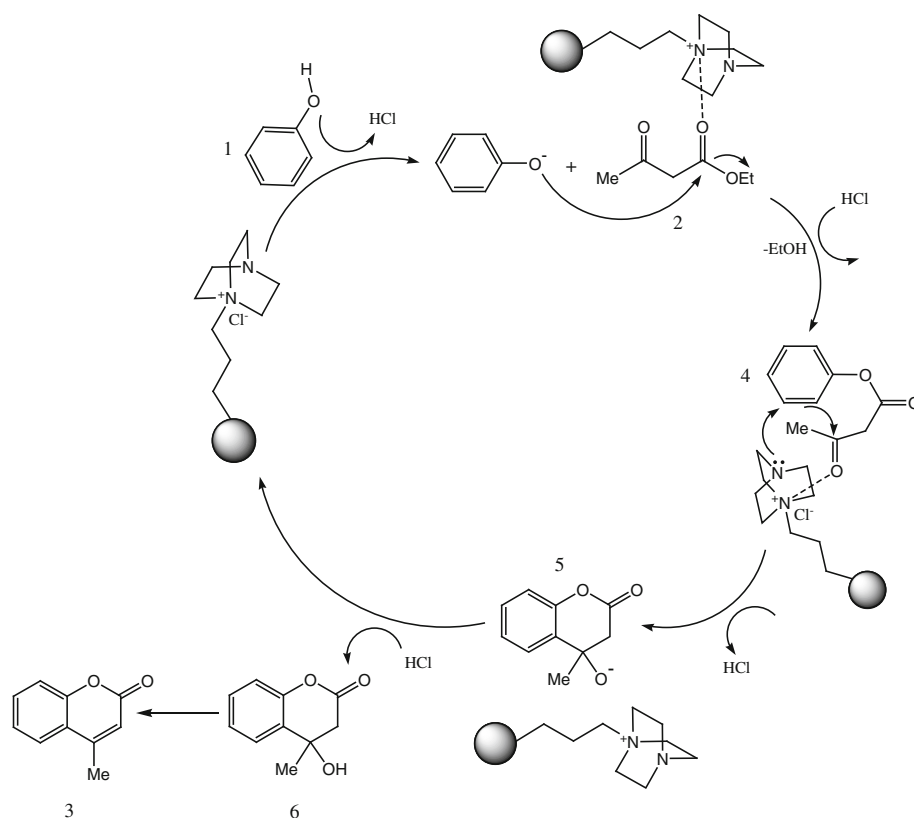
developing research area. The main objectives are solvent-free conditions, a rapid (immediately) and easy immobilization technique, and low-cost precursors for the preparation of highly active and stable MPs with high densities of functional groups. Furthermore, applying the young area of magnetite particles which are intrinsically not magnetic, but can readily be magnetized by an external magnet, can have a positive effect on high activity on one hand and separation and recycling on the other hand.

References

1. C.L. Zhu, M.L. Zhang, Y.J. Qiao, G. Xiao, F. Zhang, J. Phys. Chem. C **114**, 16229 (2010)
2. J.Q. Hu, Y. Bando, J.H. Zhan, D. Golberg, Appl. Phys. Lett. **85**, 3593 (2004)
3. B. Liu, H.C. Zeng, Small **1**, 566 (2005)
4. J. Cao, J.Z. Sun, J. Hong, H.Y. Li, H.Z. Chen, M. Wang, Adv. Mater. **16**, 84 (2004)
5. X.M. Sun, Y.D. Li, Angew. Chem. Int. Ed. **43**, 597 (2004)
6. Q.B. Wang, Y. Liu, Y.G. Ke, H. Yan, Angew. Chem. Int. Ed. **47**, 316 (2008)
7. J.L. Lyon, D.A. Fleming, M.B. Stone, P. Schiffer, M.E. Williams, Nano Lett. **4**, 719 (2004)
8. P.P. Yang, Z.W. Quan, Z.Y. Hou, C.X. Li, X.J. Kang, Z.Y. Cheng, J. Lin, Biomaterials **30**, 4786 (2009)
9. M. Zhang, Y.P. Wu, X.Z. Feng, X.W. He, L.X. Chen, Y.K. Zhang, J. Mater. Chem. **20**, 5835 (2010)
10. S.S. Liu, H.M. Chen, X.H. Lu, C.H. Deng, X.M. Zhang, P.Y. Yang, Angew. Chem. Int. Ed. **49**, 7557 (2010)
11. Y.H. Won, D. Aboagye, H.S. Jang, A. Jitianu, L.A. Stanciu, J. Mater. Chem. **20**, 5030 (2010)
12. Y. Li, J. S. Wu, D. W. Qi, X. Q. Xu, C. H. Deng, P. Y. Yang, X. M. Zhuang, Chem. Commun. 564 (2008)
13. B. Baghernejad, Eur. J. Chem. **1**, 54 (2010)
14. J. Wu, X. Sun, Y. Li, Eur. J. Org. Chem. 4271 (2005)
15. M. Heravi, F. Derikvand, M. Ghassemzadeh, B. Neumuller, Tetrahedron Lett. **46**, 6243 (2005)
16. K. Asadolah, M.M. Heravi, R. Hekmatshoar, Rus. J. Org. Chem. **45**, 1110 (2009)
17. Y.-J. Shi, G. Humphrey, P.E. Maligres, R.A. Reamer, J.M. Williams, Adv. Synth. Catal. **348**, 309 (2006)
18. L. Cecchi, F. De Sarlo, F. Machetti, Tetrahedron Lett. **46**, 7877 (2005)
19. M.M. Heravi, R. Hekmat Shoar, L. Pedram, J. Mol. Catal. A: Chem. **231**, 89 (2005)
20. M. Selvaraj, B.R. Min, Y.G. Shul, T.G. Lee, Micropor. Mesopor. Mater. **74**, 157 (2004)
21. J.F. Pan, K. Chen, Tetrahedron Lett. 45, 2541 (2004)
22. P. Radha Krishna, A. Maryurani, V. Kannan, G.V.M. Shasma, Tetrahedron Lett. 45, 1183 (2004)